



## LJMU Research Online

**Vereschaka, AA, Vereschaka, AS, Batako, ADL, Mokritskii, BJ, Aksenenko, AY and Sitnikov, NN**

**Improvement of structure and quality of nanoscale multilayered composite coatings, deposited by filtered cathodic vacuum arc deposition method**

<http://researchonline.ljmu.ac.uk/id/eprint/6203/>

### Article

**Citation** (please note it is advisable to refer to the publisher's version if you intend to cite from this work)

**Vereschaka, AA, Vereschaka, AS, Batako, ADL, Mokritskii, BJ, Aksenenko, AY and Sitnikov, NN (2017) Improvement of structure and quality of nanoscale multilayered composite coatings, deposited by filtered cathodic vacuum arc deposition method. *Nanomaterials and Nanotechnology*. 7.**

LJMU has developed [LJMU Research Online](#) for users to access the research output of the University more effectively. Copyright © and Moral Rights for the papers on this site are retained by the individual authors and/or other copyright owners. Users may download and/or print one copy of any article(s) in LJMU Research Online to facilitate their private study or for non-commercial research. You may not engage in further distribution of the material or use it for any profit-making activities or any commercial gain.

The version presented here may differ from the published version or from the version of the record. Please see the repository URL above for details on accessing the published version and note that access may require a subscription.

For more information please contact [researchonline@ljmu.ac.uk](mailto:researchonline@ljmu.ac.uk)

<http://researchonline.ljmu.ac.uk/>

# Improvement of structure and quality of nano-scale multi-layered composite coatings, deposited by filtered cathodic vacuum arc deposition method

Alexey A. Vereschaka (1), Anatoly S. Vereschaka (1), Andre D.L. Batako (2), Boris J. Mokritskii (3), Anatoliy Y. Aksenenko (1), Nikolay N. Sitnikov (4,5)

(1) Moscow State Technological University STANKIN, (2) Liverpool John Moores University (LJMU), (3) Komsomolsk-na-Amure State Technical University, (4) Federal State Unitary Enterprise "Keldysh Research Center", (5) National Research Nuclear University MEPhI (Moscow Engineering Physics Institute)

**Abstract:** The paper studies the specific features of cathode vacuum arc deposition of coatings used in production of cutting tools. The detailed analysis of the major drawbacks of arc-PVD methods has contributed to the development of the processes of filtered cathodic vacuum arc deposition (FCVAD) to form nano-scale multi-layered composite coatings (NMCC) of increased efficiency. This is achieved through the formation of nano-structure, increase in strength of adhesion of coating to substrate up to 20%, reduction of such dangerous coating surface defects as macro- and microdroplets up to 80%. Presents the results of the studies of various properties of developed NMCC. The certification tests of carbide tool equipped with cutting inserts with developed NMCC compositions in longitudinal turning (continuous cutting) and end symmetric milling, and intermittent cutting of steel C45 and hard-to-cut nickel alloy of NiCr20TiAl showed advantages of tool with NMCC as compared to the tool without coating. The lifetime of the carbide inserts with developed NMCC based on the system of Ti-TiN-(NbZrTiCr)N (FCVAD) was increased up to 5-6 times in comparison with the control tools without coatings and up to 1.5-2.0 times in comparison with NMCC based on the system of Ti-TiN-(NbZrTiCr)N (standard arc-PVD technology).

**Keywords:** PVD, wear resistance coating, cutting tool, tool life, turning, milling

## 1. Introduction

The global industrial production more and more often apply the processes to increase performance characteristics of various products by deposition of modifying multi-layered composite coatings. The most impressive positive results are demonstrated by edge cutting tools with coatings of modern generation in the machining of a variety of structural materials, including materials commonly referred to as "hard-to-cut materials" [1-14]. In particular, up to 85-90% of carbides cutting tools are produced with coatings of various compositions, architectures and properties [14]. The increased performance of coated cutting tool is achieved due to:

(i) better balance between brittle and plastic strength of the composition of "tool material-coating";

(ii) reduction of the level of thermomechanical stresses acting on the cutting wedge of the tool during cutting;

(iii) improvement of the thermal state of the cutting tool system, which results in the increase in resistance of the cutting tool wedge to brittle and plastic failure and reduction in tool wear rate [1-8][10][12-14];

Different types of tools made of high speed steels and carbides with coatings of modern generation are characterized by higher performance exceeding the lifetime of standard uncoated tool by 1.5-8 times, and they can increase the material removal performance due to the increase in cutting speed by 20-60% [1][2][4-6][8][12-16].

The processes of vacuum-arc deposition of coatings, referred to as Metal Vapor Vacuum Arc (MeVVA), are widely used in the practice of tool production, being the most adaptive processes for the implementation of new principles for formation of coatings of various functional purposes, relevant to concepts of gradient, metastable, discrete, multi-component, multi-layered, or superlattice [1][2][6][8][17-20]. MeVVA processes are based on generation of substance with cathode spot of vacuum arc of high-current, low-voltage discharge, emerging only in pairs of the cathode material. MeVVA processes are characterized by high performance of coating deposition, ten times higher than performance of, for example, CVD processes. This can be explained by the possibility for acceleration of high-ionized flow by applying a negative potential (relative to camera body) to the substrate, as well as by the possibility for significant increase in density and homogeneity of the plasma stream by means of special magnetic accelerating systems (Hall accelerators)[1][15][17][18][19]. MeVVA processes are implemented in a wide range of temperature changes with short duration of the process, which eliminates the thermal softening of all tool materials and allows considering these processes as universal. Furthermore, MeVVA processes provide high adhesion between the coating and the substrate, they are characterized by good reproducibility and alternatives for automation and are environmentally friendly.

Meanwhile, MeVVA processes are also characterized by organic drawbacks, as follows [1][6][21][22]:

- (i) formation of macro- and microparticles of the cathode material during plasma generation, especially for metals with relatively low atomic weight and density of (Ti, Al, etc.), which is a dangerous coating defect. These macro- and microparticles reduce the operational efficiency of coated products, especially if they are located at the boundaries of the system "substrate-coating" or on the coating surface;
- (ii) combination of processes of thermal activation (heating) and ionic cleaning of product surface prior to application of coating, which, on the one hand, can result in electroerosion of its cutting edges (because of stochastic formation microarcs), and on the other hand, in sharp deterioration of the coating surface because of insufficiently complete ion cleaning;
- (iii) effect of "focus" of the plasma flow, affecting the formation of the highest-quality coating only when the plasma flows perpendicularly to the product surface, and that results in the need for complex motion of the tool relative to the plasma flow in the station chamber (as a rule, a planetary or double planetary rotation)

## **2. Methods to improve structure and quality of functional nano-structured coatings for cutting tools, deposited by MeVVA method**

At present, the basic trends for improvement of the MeVVA processes relate to:

- (i) development of processes and devices for the filtration of vapor-ion stream in order to separate macro- and microparticles;
- (ii) creation of devices for quenching microarc and prevention of electroerosive etching of cutting edges and working surfaces of the tool;
- (iii) development of processes to form nano-structured coatings of various compositions and architectures;
- (iv) development of the combined processes for modification of working surfaces of the tool (laser-assisted deposition of coatings, deposition of coating with high-energy ions with power of about 10-200 keV, combined treatment with plasma, stimulated by electric discharge, followed by coating deposition, etc.).

Following the analysis of features of the plasma generated by vacuum arc spots, the following can be noted [15][17][18][21-27]:

- (i) plasma contains a certain amount of different neutral particles;
- (ii) kinetic energy of the ions is relatively high (20-100 eV) and is higher than the energy  $eU_0$  of cathode-anode potential drop, where  $U_0$  - arc voltage;
- (iii) electrical current moves up to 8% of ions;

(iv) electric field in the plasma is extremely weak.

The cathode spot is of small diameter (from  $10^{-8}$  up to  $10^{-4}$  m) and is an intense source of plasma with current density of about  $(10^6-10^{12}) \text{ A m}^{-2}$ . Spot motion speed is determined by the coefficients, dependent on a number of factors, including the properties of the cathode material, the residual vacuum and the parameters of external magnetic fields. The rate of erosion of the cathode depends on the state of its surface and can vary significantly depending on the presence of contaminants or oxide films.

The flow ejected from the cathode surface consists of a mixture of vapor and ion particles (main component), macro- and microparticles (droplet phase). The ability to eject the highly ionized plasma flows (up to 90-95%) in vacuum space is the reason for the widespread use of systems with arc plasma sources, since it provides directional control over the parameters of coating deposition on the activated surface of the substrate material [1][18][23][24][26]. The emission of ions is characterized by the energy, the discharge state and the degree of ionization.

Positively charged ions, ejected by the cathode spots from the cathode surface, are able to reach the anode and possess the energies much exceeding the energies projected at certain potential difference between the anode and the cathode [7-9][17]. It is found out that when the cathode-anode potential drop reaches 10-30 V, the energy level of the ions emitted from the cathode surface is about 13-50 eV per discharge [9]. To explain this phenomenon, two hypothetical theories were suggested for the mechanisms of formation of ions with the energies higher than the energies of the cathode-anode potential drop. According to the theory of the potential maximum [9][17], the ions, which are formed as a result of electron-atom collisions, are ejected toward the anode from the area of the positive ion cloud, instantly appearing directly above the spot of vacuum arc. In the area of the ion cloud, the maximum peak potential is formed above the cathodic plane, and if this figure exceeds the cathode potential by approximately 50 V, it is sufficient to accelerate the ions up to the energies that are typically registered by experiments (Fig. 1).

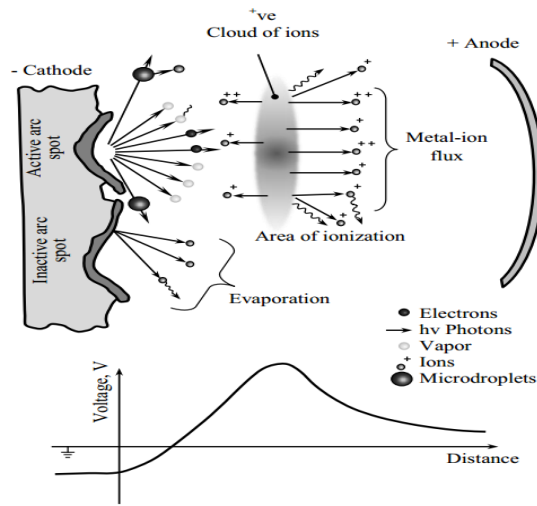


**Figure 1.** Schematic physical model of the emission of particles from the surface of the active cathode spot of the arc discharge and high voltage distribution in the area near the cathode

The gas dynamic theory [18][28] explains the increase in the ion energy by the momentum transfer from the flow of electrons to the ions through collisions. It should be noted that the precise model of the ion acceleration mechanism is under discussion and the both above mechanisms are so far hypothetical.

The cathode spot and the interelectrode area are also a source of intense photon emission [28]. The detailed spectroscopic studies of these areas in the direction of the normal surface of the cathode showed the presence of neutral particles with energies of about 5 eV and ions with energies of 50-60 eV. The instability of photon flow from neutral particles, registered during measurements, as compared to the stability of the measurements of flow of ionized particles, indicates that the vapor can also be formed within the extended area, which actually is not limited by the cathode spot. Evaporation can also occur in areas with molten metal signs created by migrating cathode spots. The charge state of ions  $Z$  is evaluated statistically and under repeated measurements, that determines very high degree of their charge (about  $Z = 6$ ) [8]. The degree of ionization depends strongly on the properties of the evaporated cathode material. For example, at evaporation of Ti under high vacuum, the degree of ionization is about 0.7, and at evaporation of TiN under residual nitrogen pressure  $p_N=0.1-1.5$  Pa about 0.85. The particles, ejected by the cathode spot of vacuum-arc discharge, include macro- and microdroplet component of the cathode material with the diameters of about 0.1-100  $\mu\text{m}$  (Fig. 2) [1][2][5][21][22][25][26].

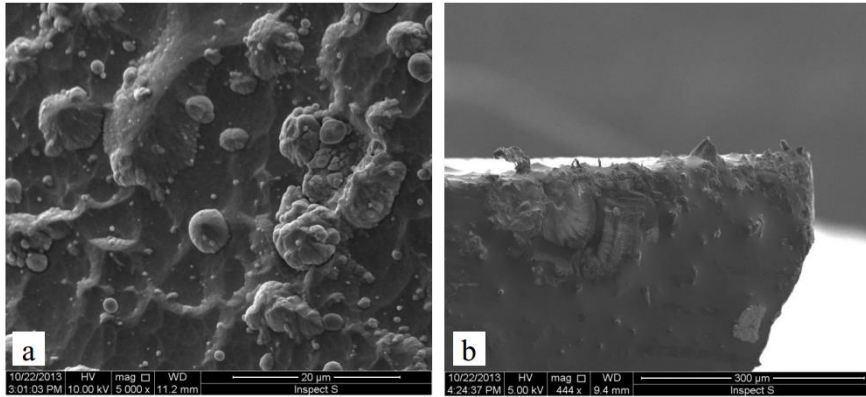


**Figure 2.** Widespread coating defects appearing through the use of the MeVVA standard processes. a – formation of micro- and macroparticles (with diameter of 0.5-9.0  $\mu\text{m}$ ), b – electroerosion (violation of microgeometry) of the cutting edge as a result of the formation of microarcs.

Generated particles can appear over the entire coating, at boundaries of the interface of "coating-substrate" and on its surface, into contact with cut chips. Micro- and macroparticles, which appear on the boundaries of the interface of "coating-substrate" and on its surface, are particularly dangerous. In one case, it can result in partial or complete delamination of the coating because of the sharp decline in the strength of adhesion to the tool material, and in the second case in the increase in the propensity to adhesion to the material being machined, formation of strong adhesive bonds between them, emergence of large centres of coating failure, and sharp increase in wear rate for tool contact areas. Typical coating defects, which decrease their efficiency, are shown in Fig. 3-5.

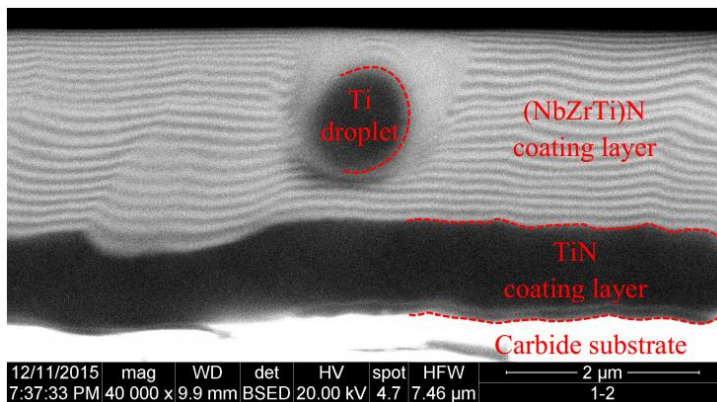


**Figure 3.** Typical coating defect in the form of failure of integrity of coating of Zr-ZrN-ZrCrAlN because of penetration of Al microparticle on the boundary of the interface "adhesive underlayer-intermediate layer" (microparticle diameters are about 11  $\mu\text{m}$ ). 1 – adhesion layer (Zr), 2 – intermediate layer (ZrN), 3 – wear resistant layer (ZrCrAlN)

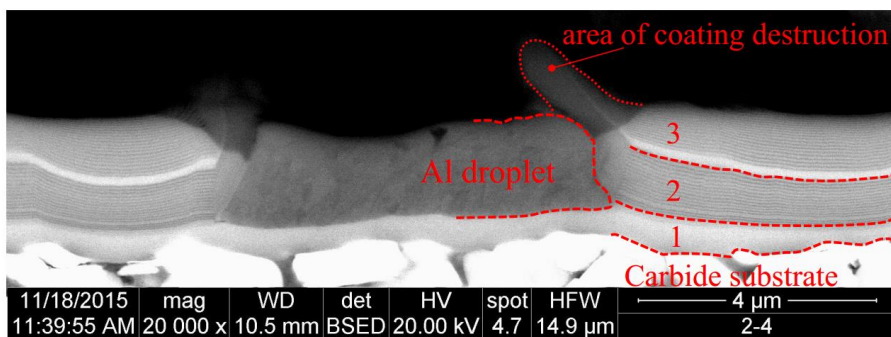


**Figure 4.** Coating defect in the form of Ti microdroplet embedded into the structure of coating of Ti-(NbZrTi)N (microparticle diameter is about 1.5  $\mu\text{m}$ , thickness of nanolayer is 40-70 nm).

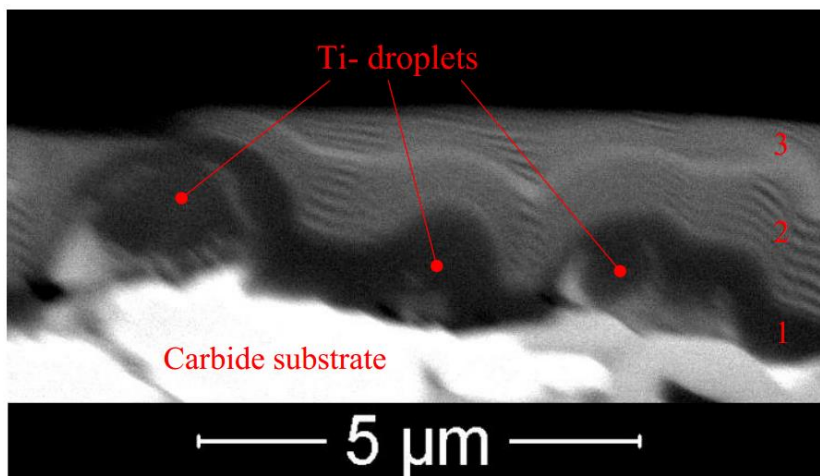


**Figure 5.** Dangerous coating defect in the form of Ti microdroplets on the boundary of the interface "coating-substrate" (microparticle diameter is 1-2.5  $\mu\text{m}$ , thickness of coating nanolayers is 40-70 nm). 1 – adhesion layer (Ti), 2 – intermediate layer (TiCrN), 3 – wear resistant layer (TiCrAlN)

Analyzing typical coating defects arising from the use of standard arc-PVD processes MeVVA, it may be noted that the problem of reducing the number of micro - and macro droplets, is one of the most important tasks of perfection for coating deposition technologies on the cutting tools. Recently research to improve the quality of coatings by reducing the number of micro - and macro droplets of cathode material at deposition of coatings are conducted, which result are presented in publication [10][18][21-25][29-31].

In this context, the challenge of reducing the formation intensity and the number of macro- and microparticles is one of the most important tasks of improving the technology of deposition of coatings through the MeVVA methods. Recently, a large number of studies

were carried out concerning the improvement of coating quality by reducing the number of micro- and macro droplets of cathode material during deposition of coatings.

To understand the main reasons for the generation of droplets, let us briefly examine the mechanism of their formation during the process of coating deposition. The droplets are ejected from the cathode surface at a slight angle to the surface with a pronounced peak in the distribution at an angle of about 20°. The distribution of sizes of ejected droplets obeys the exponential law, and the amount of particles in the distribution increases when their size decreases. The extremum distribution corresponds to the maximum number of droplets with diameters of 0.1-2.0 µm. Rate of erosion of macro droplets  $W_{mp}$  can be estimated by the formula:

$$W_{mp} = W_{total} - \frac{F \cdot m_i}{eZ}$$

where  $W_{total}$  – full cathode erosion rate;  $F$  – component of the ion current ( $\sim 0,1$ );

$m_i$  – ion mass;  $eZ$  – average state of ion charge.

The intensity of the droplets ejection from the cathode surface increases with the decrease in the ultimate melting temperature of metal and erosion rate  $W_{mp}$ . Upon evaporation of the refractory materials and intense cooling of the cathode, the amount of formed of micro- and macro droplets decreases considerably and reaches less than 1% of the total mass of the erodible cathode material.

It is found out that the droplets size decreases with the increase in nitrogen partial pressure, and it is caused by the passivation of (Ti) cathode surface with layer of TiN, resulting in the increase in the melting point of the cathode surface from 1675°C (Ti) up to 2950°C (TiN). Droplets ejection rate is in the range 0.1-800 m sec<sup>-1</sup>, depending on the mass of droplets [17]. Several papers are devoted to the modeling of the process of formation of micro- and macro droplets in order to understand the speed and angular distribution of droplets with respect to the cathode spot. The paper [22] proposes a model based on the expansion of plasma in which ions from the ion cloud (above the cathode spot) accelerate towards the molten surface of the active cathode spot. Reactive force of the vapor stream exerts pressure on the molten metal which is pushed to edge of crater, and that results in the observed spatial distribution. Using the proposed model, it is possible to predict the speed of injected droplets, for example, copper droplets, within 20-100 m sec<sup>-1</sup>.

The second of the proposed models of formation of micro- and macro droplets [28] is based on the concept of the explosive nature of the ion emission. The model assumes that the electron emission is concentrated on local formations projecting from the surface of the cathode. Such formations are quickly warmed up by electrons, and that eventually results in an outburst of such formations at peak pressures of about  $2 \cdot 10^{10}$  Pa. The outburst results in the formation of numerous surface defects and the formation of other cathode spots, whereby the above process is repeated. More effective approaches to the challenge to reduce

the amount of emitted particles require a modification of plasma source and development of special filters.

As a result of the conducted studies [18], it is found out the vacuum arc spot of high-current low-voltage discharge generate micro- and macroparticles of droplets from the liquid phase during the formation of erosion craters on the surface. The formation of solid fragments (droplets) of the cathode material occurs because of thermoelastic stresses arising in the material in excess of the limit of its strength. The simplest means to reduce the amount of droplets in the vacuum-arc coating synthesis are as follows:

- (i) reduction of the temperature of the cathode surface by its intense cooling;
- (ii) reduction of the arc current in order to reduce the density of ion flow;
- (iii) accurate placement of the substrate (product) surface relative to the surface (evaporated plane) of the cathode.

The influence of substrate bias and hydrogen/nitrogen incorporation on the optical properties of tetrahedral amorphous carbon (ta-C) films, deposited by S bend filtered cathodic vacuum arc (FCVA) process, is reported in [32].

Filtered plasma arc sources relate to the class of sources (usually with the use of DC), which use a variety of devices reducing the amount of micro- and macroparticles of the plasma flow (Fig. 6). The simplest method to reduce the amount of droplets in the condensable coating is to take advantage of spatial distribution of droplets emission and substrate placement to such position in the vacuum chamber to ensure it is not on a straight line to the cathode. The effect of the droplets filtration can be provided by placing a screen between the substrate and the arc source [21] (Fig. 6 a). In this case, the substrate and the screen are offset from each other in order to move the plasma around the screen towards the substrate. The generated droplets are trapped on the medial side of the screen and do not reach the substrate surface. The principal drawback of this method is a sharp decrease in condensate deposition rate on the substrate, although 2-3  $\mu\text{m}\cdot\text{hour}^{-1}$  are high enough ( $I_a=80\text{ A}$ , diameter 125 mm – for controlled arc, diameter 63 mm – for stochastic arc). The controlled arc significantly reduces the amount of large macroparticles (with a diameter of  $>100\ \mu\text{m}$ ), especially in nitrogen  $\text{N}_2$  atmosphere. External solenoidal devices are also used to enhance the growth of ion source evaporation. Such sources are used to sputter material from the surface of a cooled target and subsequent deposition on the surface of the substrate [30]. It is found out that when Ti-, Al- and Nb-based coatings are deposited, super small grains are formed with virtually no formation of macro- and microparticles. The deposition rate was varied in the range of 2-6  $\mu\text{m}\ \text{hour}^{-1}$ , depending on the target material and the bias potential. Authors of the paper [22] studied the influence of magnetic fields on parameters of vacuum-arc evaporation, with magnetic fields applied by a solenoid mounted directly in front of cathode (Fig. 6 b). When Ti evaporates, the solenoid field enhances the degree of ionization of the ion flow up to 100% with an average state of ion charge of 2.08. The deposition rate was varied in the range of 2-6  $\mu\text{m}\cdot\text{hour}^{-1}$ , depending on the cathode material and the bias potential.

A source of the "joint" type (Fig. 6, d) [23], a source with the plasma flow deviation (Fig. 6 e) [29], and a source with emission grid and hollow cathode open in the direction of the grid (Fig. 6 f) [24] are used.

The paper [25] proposes a design of toroidal ion source, in which charged particles are deflected by powerful magnetic field, and neutral micro- and macroparticles are trapped by special device. The filtering source consists of a plasma duct (deflector), which is a part of a torus with an angle of  $120^\circ$ . The inner diameter of the deflector is 200 mm, and an electromagnetic coil is placed at its outer side. At the deflector inlet, a cathode assembly is located with cathode mounted thereon, which is shifted from the centre of the deflector so as to be located relative to the centre of the torus at radius  $R_0 = \sqrt{(rR)}$ , where  $r$  and  $R$  minor and major radii of the deflector walls, respectively.

Therefore, when current is passed through the coil inside the deflector, uniform magnetic field is created along the entire length.

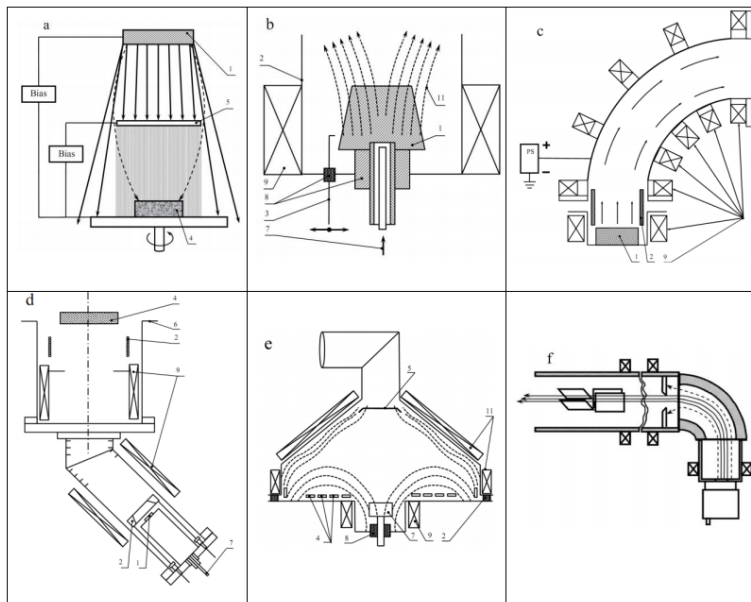


**Figure 6.** Sources with filtration of plasma flow: shade sources (a) [21]; extending source with a field coil (b) [22]; sources with filtration of plasma particles (c) [25]; sources of "joint" type (d) [23]; source with plasma flow deviation (e) [29]; source with emission grid and hollow cathode open in the direction of grid (f) [24]. 1 – cathode; 2 – anode; 3 – trigger; 4 - substrate; 5 – cathode case; 6 – wall of vacuum chamber; 7 – cooling system; 8 – insulator; 9 – magnetic coil; 10 – magnetic field lines.

At the opposite end of the deflector, the anode of arc charge is located, which can be represented by walls of the vacuum chamber, and positive or negative voltage is supplied to the body of the deflector. Therefore, when current is passed through the coil, a magnetic

field uniform along its length is formed inside the deflector. The magnitude of the magnetic field at the centre line of the torus is about 600 G. The arc discharge is ignited between the cathode and the anode and allows the passage of the electron current through the plasma arc formed inside the deflector. Since the electronic component of plasma is magnetized, then magnetic field lines, crossing the cathode and passing near the axis of the deflector, take the potential close to the cathode potential, and the power lines near its walls - the wall potential. Therefore, the plasma creates an electric field, perpendicular to the walls of the deflector, which provides the ion drift from the walls or to the walls of the deflector depending on the polarity and magnitude of the voltage applied. Thus, the ionized plasma component is transported along the magnetic field lines through the deflector to the exit in the vacuum chamber, whereas the particles and the neutral plasma component are deposited on the lamella traps mounted on the walls of the deflector (Fig. 6 c). Besides, this device can act as a plasma stream accelerator and serve as a source of electrons for thermal activation of the material adjacent to the working surfaces of the tool and a source of highly charged ions of gas (e.g. nitrogen) for stimulated thermochemical machining of the tool. Such processes and technologies based thereon are referred to as the filtered cathodic vacuum arc deposition (FCVAD). From the above, it is possible to propose more active introduction of the systems of vapor-ion flow filtration for separation of macro- and microparticles and, consequently, improvement of the performance properties of coatings. While maintaining the advantages of the MeVVA method, these systems can eliminate such a drawback of this method as the formation of macro- and microparticles of the cathode material during the plasma generation, especially for metals with relatively low atomic weight and density (Ti, Al, etc.).

### **3. Architecture of developed nano-scale multi-layered composite coatings.**

Coatings have a dual nature as an "intermediate technology medium" between the tool and the workpiece materials. Using this concept of dual nature, functional requirements for coatings for cutting tools were derived to prove the concept of multilayer composite coatings with nano-scale structure [2-7].

To modify the surface properties of cutting tools, it is proposed to use three-layered nano-scale multi-layered composite coatings (NMCC), consisting of the outer wear-resistant layer 1 in contact with the material being machined, the intermediate layer 2 in simultaneously contact with the outer layer 1, and the adhesive sublayer 3 in contact with tool material (substrate) (Fig. 7).

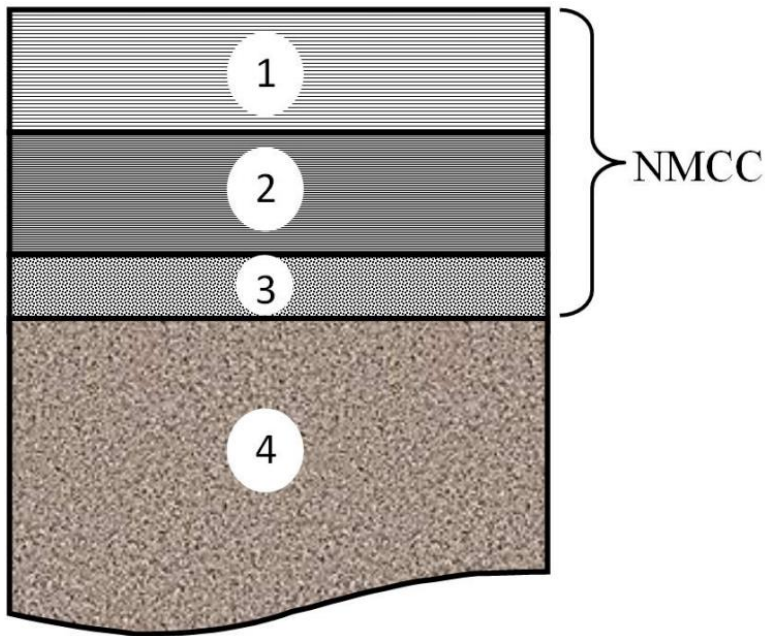


**Figure 7.** Three-layered architecture of NMCC for cutting tool: 1 – wear-resistant layer; 2 – intermediate layer; 3 – adhesive sublayer; 4 – tool material (substrate).

Composition, architecture, structure and properties of every layer of NMCC in the process of modification of properties of tool material should improve wear resistance of tool material under specified conditions of tool operation. Use of NMCC can simultaneously solve the problem associated with the dual nature of coatings on contact areas of cutting tool that acts as an intermediate technological environment between tool material and processed material. Actually, NMCC can simultaneously improve wear resistance of contact areas of cutting tool by reducing physical and chemical activity of tool material, reducing adhesion with regard to processed material and reducing the thermo-mechanical stresses acting on the tool contact areas (function of outer layer 1 NMCC), and it simultaneously provides high adhesion strength with tool material (function of adhesive sublayer 3 NMCC) [2-7]. Intermediate layer 2 performs an extremely important function: in addition to providing strong adhesion with the layers 1 and 3, it blocks diffusion in the system " tool material - workpiece material " and reduces the intensity of the heat flows from the frictional heat sources to the cutting tool and surface of the workpiece under machining.

For the formation of coatings modifying the properties of cutting tools and forming multilayer composite system with nano-scale structures, this study used the technology based on the process of FCVAD. This technology allows forming coatings with strong adhesion to substrate, high density, and hardness, and that provides a significant increase in efficiency of cutting tools.

The technology of applying NMCC included three main stages:

- (i) pre-treatment of samples of carbide cutting inserts (for turning tools and face milling cutters);
- (ii) following fine ionic cleaning and thermal activation of the inserts directly at the station chamber;
- (iii) actual deposition of coatings.

The parameters used at each stage of the deposition process of nano-scale multi-layered composite coatings (NMCC) are shown in Table 1.

Table 1. Parameters of stages of the technological process of deposition of NMCC.

Process	$p_N$ (Pa)	$U_b$ (V)	$I_{Al}$ (A)	$I_{ZrNb}$ (A)	$I_{Ti}$ (A)	$I_{Cr}$ (A)
Pumping and heating of vacuum chamber	0.06	+20	120	80	65	75
Heating and cleaning of products with gaseous plasma	2.0	100 DC / 900 AC f = 10kHz, 2:1	80	-	-	-
Deposition of coating	0.36	-80-160 DC	160	135-170	55	70
Cooling of products	0.06	-	-	-	-	-

where  $I_{Ti}$  = current of titanium cathode,  $I_{Al}$  = current of aluminum cathode,  $I_{ZrNb}$  = current of zirconium-niobium cathode,  $I_{Cr}$  - current of chromium cathode,  $p_N$  = gas pressure in chamber,  $U$  = voltage on substrate.

During the process of coating deposition, the following cathodes were used:  
Ti 99.8%, Al 99.9%, (Zr 80%+Nb19.5%), Cr 99.9%.

## 4. Results and discussion

### 4.1. Studies of physical and mechanical properties of NMCC

Surface morphology and structure of transverse section of designed NMCC are shown in Fig. 8.

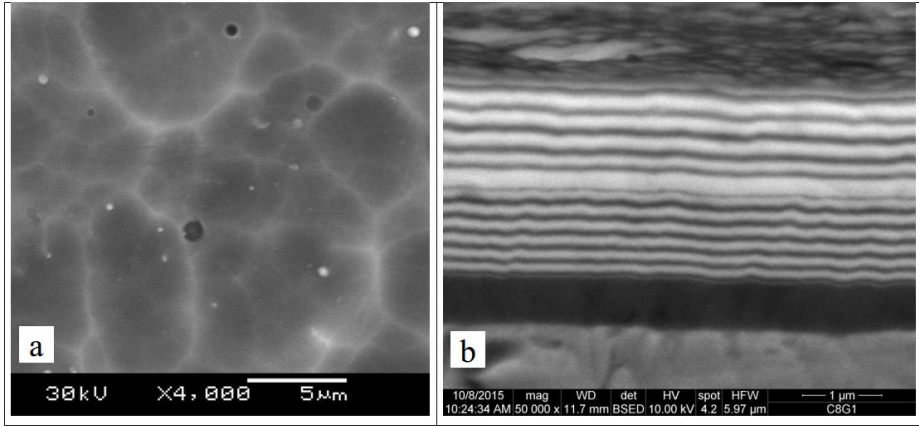


**Figure 8.** NMCC based on system of Ti-TiN-(NbZrTi)N, obtained in the use of the FCVAD technology: a - surface morphology; b - microstructure on transverse section.

The results of the study of component composition of NMCC, obtained by X-ray microanalysis, are shown in Table 1. It is found out that, depending on the parameters of the FCVAD deposition process, the following NMCC composition is synthesized: 16 – 18 atm. % Cr, 16 – 17 % atm. Ti, 19 – 24 atm. % Zr, 42 – 47 atm. % N, 1-2 atm. % Al and 2-3 atm. % Nb.

Table 2. Chemical composition of NMCC based on the system Ti-TiN-(NbZrTiCr)N.

Parameters of FCVAD process		Content of elements in FCVAD, % atm.				
		Ti	Cr	Zr	Nb	N
$I_{NbZr} = 130 \text{ A}$	$U_b = -80 \text{ V}$	17	16	19	1	47
$I_{NbZr} = 130 \text{ A}$	$U_b = -100 \text{ V}$	17	16	19	1	47
$I_{NbZr} = 130 \text{ A}$	$U_b = -120 \text{ V}$	17	17	20	1	45

$I_{\text{NbZr}} = 165 \text{ A}$	$U_{\text{b}} = -120 \text{ V}$	16	15	24	2	43
$I_{\text{NbZr}} = 125 \text{ A}$	$U_{\text{b}} = -160 \text{ V}$	17	18	20	2	43

The study has revealed considerably strong influence of the parameters of the synthesis process on their properties. In particular, when current of NbZr cathode arc increased from 135 up to 170 A, the content of niobium and zirconium in the coating increased from 2.7 to 3.13%, respectively, with corresponding reduction in concentrations of other elements.

The growth of bias potential on carbide substrate  $U_{\text{b}}$  from - 80 to - 160 V, which increases the energy of deposited ions, reduces the nitrogen content from 47 down to 42% (atomic). This result apparently relates to high nitrogen dispersibility as the lightest element in the composition of NMCC, by heavy metal ions (Cr, Zr, Nb).

The study of phase composition of NMCC Ti-TiN-(NbZrTiCr)N by the method of X-ray diffractometry, the fragments of which are shown in Fig. 9.

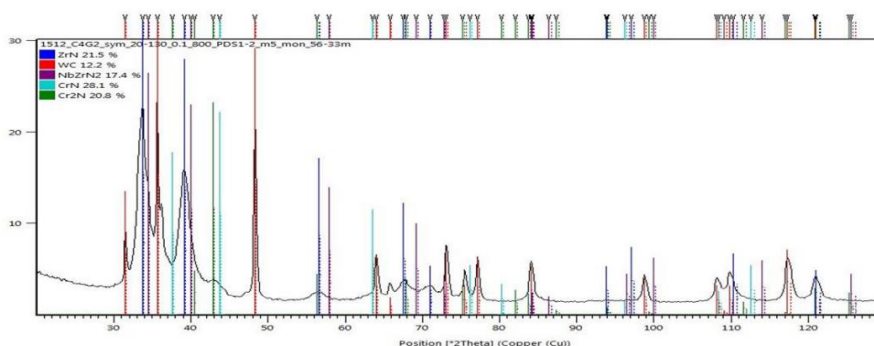


**Figure 9.** Plot of diffraction patterns of carbide sample with NMCC on the base of Ti-TiN-(NbZrTiCr)N

The hardness (HV) of coatings was determined by measuring the indentation at low loads, according to the method of Oliver and Pharr [33][34], which was carried out on a Micro-Hardness Tester (CSM Instruments) micro-indenter at a fixed load of 300 mN. The penetration depth of the indenter was monitored so that it did not exceed 10–20% of the coating thickness to limit the influence of the substrate. The nanomechanical properties of coatings and analysis of the nanoscratching processes at low loads to obtain quantitative analysis, the comparison of their elastic/plastic deformation response, and nanotribological behavior of coatings presented in [35-37].

The results of the study of physical-mechanical properties of developed NMCC based on Ti-TiN-(NbZrTiCr)N are shown in Table 2.

Table 3. Physical and mechanical properties of NMCC.

Parameters of deposition		H, GPa	E, GPa	H/E	H <sup>3</sup> /E <sup>2</sup> , GPa	Wp, %
U <sub>b</sub> = -80 V	n = 1 rev/min	28,1	440	0,06	0,11	58
U <sub>b</sub> = -100 V	n = 1 rev/min	29,5	460	0,06	0,12	57
U <sub>b</sub> = -120 V	n = 1 rev/min	32,3	490	0,07	0,14	55
U <sub>b</sub> = -160 V	n = 1 rev/min	25,9	430	0,06	0,09	61
U <sub>b</sub> = -120 V	n = 2 rev/min	36,6	580	0,06	0,15	56
U <sub>b</sub> = -120 V	n = 3 rev/min	34,5	570	0,06	0,13	53

Following the analysis of the obtained results, the following can be noted. When bias potential U<sub>b</sub> applied to the carbide substrate increases, the hardness of NMCC on the base Ti-TiN-(NbZrTiCr)N (as example) increases from 28.1 GPa at U<sub>b</sub> = -80V and n = 1 rev/min up to 32.3 GPa at U<sub>b</sub> = -120 V and n = 1 rev/m. This is apparently a consequence of the effect of ionic hardening, the possibility of which increases with the increase in U<sub>b</sub> and, respectively, the magnify in the energy of bombarding ions. At the same time, it increases the level of microdistortions of NMCC due to deformation of the crystal lattice of the material phases. For example, for the phase on ZrN,  $e = 2.12 \pm 0.17\%$  at U<sub>b</sub> = -80 V and  $e = 2.86 \pm 0.23\%$  at U<sub>b</sub> = -120 V, and for the TiN-based phase,  $e = 1.27 \pm 0.07\%$  at U<sub>b</sub> = -80 V and  $e = 1.52 \pm 0.05\%$  at U<sub>b</sub> = -120 V. The increase in the hardness of NMCC can also relate to the compression because of the greater mobility of the atoms adsorbed on the surface and forming NMCC. With further increase of the bias potential, the hardness of NMCC

decreases to 25.9 GPa at  $U_b = -160$  V, which relates to violations of section boundaries between specific nanolayers.

The increase in the rotation speed of a carbide sample from 1 to 2 rev/min at the same bias potential  $U_b = -120$  V results in the increase in hardness of NMCC from 32.3 up to 36.6 GPa, with no reduction in toughness. In particular, it is found out that the work of plastic deformation (toughness characteristic) is almost constant and reaches 0.55 and 0.56, respectively. The marked increase in hardness is probably a consequence of the chipping of crystallites of the phases of the respective layers, caused by the decrease in the thickness of the multi-layered structure of NMCC. Meanwhile, the hardness of NMCC can grow because of the increase in the total length of the interlayer and intercrystalline boundaries, which are an obstacle for the penetration of an indenter. Further increase in the rotation speed of the sample to  $n = 3$  rev/min, despite degeneration of the multi-layered structure, is accompanied by a slight decrease in hardness down to 34.5 GPa. The latter is apparently connected with the great influence on the hardness of the crystal sizes, which are not changed and range from 3 to 6 nm.

## 4.2. Methods for study of cutting properties for carbide inserts with NMCC

This test used carbide inserts, with dimensions of  $12.5 \times 12.5 \times 4.75$  (SNUN ISO), with an edge radius  $r = 0.8$  mm. Here, a pilot batch of inserts was produced of carbides WC10XOM (WC 88%, Cr<sub>2</sub>O<sub>3</sub> 2%, Co 10 %; ISO S20-S30) and TT10K8B (WC 82%, TiC 3%, TaC 7%, Co 8% ISO S20-S30). The produced inserts were divided into three groups, the first of which (without coatings) was used as a control group, the second group of inserts was coated with complex composite coating Ti-TiN-(NbZrTiCr)N (standard MeVVA technology), and the third party of inserts was coated with the system Ti-TiN-(NbZrTiCr)N (FCVAD technology). Longitudinal turning in dry conditions was conducted maintaining the cutting speed at a specified level when the diameter of the workpiece was changed. Face milling was also carried out. The machining test were carried out on steel C45 (HB 200) and nickel-based alloy NiCr20TiAl. The following cutting parameters were used:

(i) In turning: steel C45:  $v_c = 350$  m/min;  $a_p = 1.5$  mm;  $f = 0.3$  mm/rev; nickel alloy NiCr20TiAl:  $v_c = 40$  m/min;  $a_p = 1.5$  mm;  $f = 0.3$  mm/rev;

(ii) In face milling: steel C45:  $v_c = 200-450$  m/min;  $a_p = 2.0$  mm;  $f = 0.03$  mm/tooth; nickel alloy NiCr20TiAl:  $v_c = 20-75$  m/min;  $f = 0.02$  mm/tooth;  $a_p = 2.0$  mm; Both cases used face mills  $D_{\text{mill}} = 280$  mm;  $Z = 1$ , where cutting width  $B = 80$  mm.

Cutting inserts had the following geometric configuration: for turning:  $\gamma = -8^\circ$ ;  $\alpha = 6^\circ$ ;  $k = 45^\circ$ ;  $r = 0.8$  mm; and milling:  $\gamma = -4^\circ$ ;  $\alpha = 6^\circ$ ;  $k = 75^\circ$ ;  $r = 0.8$  mm. The efficiency of cutting tools with the developed NMCC was evaluated by the time they reached a maximum flank wear  $VB_{\text{max}} = 0.4-0.5$  mm for turning and  $VB_{\text{max}} = 0.3-0.4$  mm for face milling.

### 4.3. Results of machining tests of cutting properties of carbide inserts with NMCC

The verification tests of cutting properties of inserts with developed NMCC were carried out for two fundamentally different processes: longitudinal turning (continuous cutting process with constant parameters for cross sections of cut and contact thermo-mechanical stresses during cutting in one pass) and face milling (interrupted cutting process with variable parameters for cross sections of cut and thermo-mechanical stresses during cutting).

For turning of steel, the study used inserts of carbide TT10K8B without and with NMCC. For face milling of nickel alloy, the study applied one inserts of WC10XOM with Ti-TiN-(NbZrTi)N coating.

Selection of NMCC on the basis of the composition of Ti-TiN-(NbZrTiCr)N for milling operation was justified by sufficiently balanced combination of hardness (H), modulus of elasticity (E), and toughness (WP) (see Table 2.), as well as by its high thermal stability.

The results of verification tests of inserts TT10K8B and WC10XOM (control inserts, with developed NMCC - standard MeVVA technology and FCVAD technology) for turning and milling of steel C45 and nickel alloy NiCr20TiAl are presented in Fig. 10-13. The conducted tests have revealed significant advantages of carbide tools with developed NMCC on the basis of the system Ti-TiN-(NbZrTi)N (FCVAD technology) compared to control carbide tools without coatings and developed NMCC on the basis of the system Ti-TiN-(NbZrTi)N (standard MeVVA technology).

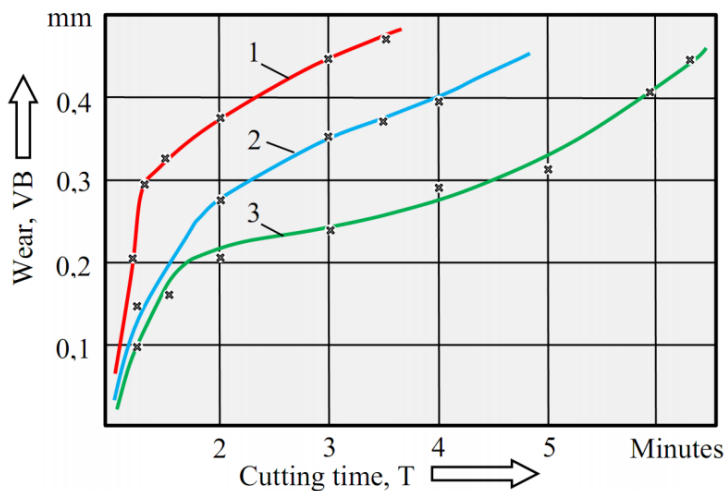


**Figure 10.** Dependence of tool wear equipped with inserts made of carbide grade TT10K8B (curve 1) with NMCC Ti-TiN-(NbZrTi)N (standard MeVVA technology) (curve 2) and with NMCC Ti-TiN-(NbZrTi)N (FCVAD technology) (curve 3) from the cutting period when turning steel C45 with  $v_c = 350$  m/min;  $a_p = 1.5$  mm;  $f = 0.3$  mm/rev

Comparison of the results of the verification tests of the cutting properties of tools of carbides WC10XOM (ISOS20-S30) and TT10K8B (ISO S20-S30) without coatings and with NMCC formed with the use of the standard MeVVA technology, with the corresponding data for carbide tools with developed NMCC (FCVAD technology). NMCC deposited on surfaces of the carbide cutting tools using the FCVAD processes sufficiently improve the tool life compared with the tool life of control carbide tool without coating or with NMCC produced with the use of the standard MeVVA technology, with fine structure and sufficiently notable imbalance of hardness and strength for all tested cutting conditions (see Fig. 10-13).

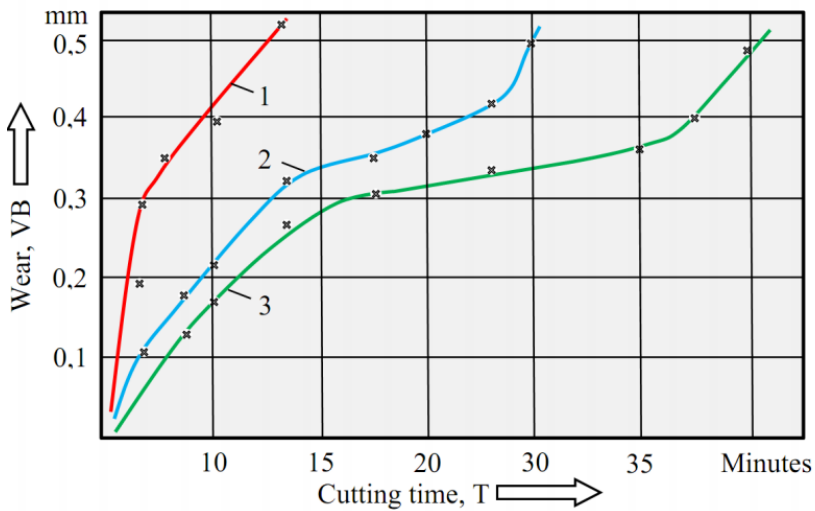


**Figure 11.** Dependence of tool wear land VB equipped with inserts made of uncoated carbide grade WC10XOM (curve 1), with NMCC Ti-TiN-(NbZrTi)N (standard MeVVA technology) (curve 2) and NMCC Ti-TiN-(NbZrTi)N (FCVAD technology) (curve 3) from the cutting period T when turning nickel alloy NiCr20TiAl with  $v_c = 40$  m/min;  $a_p = 1.5$  mm;  $f = 0.3$  mm/rev

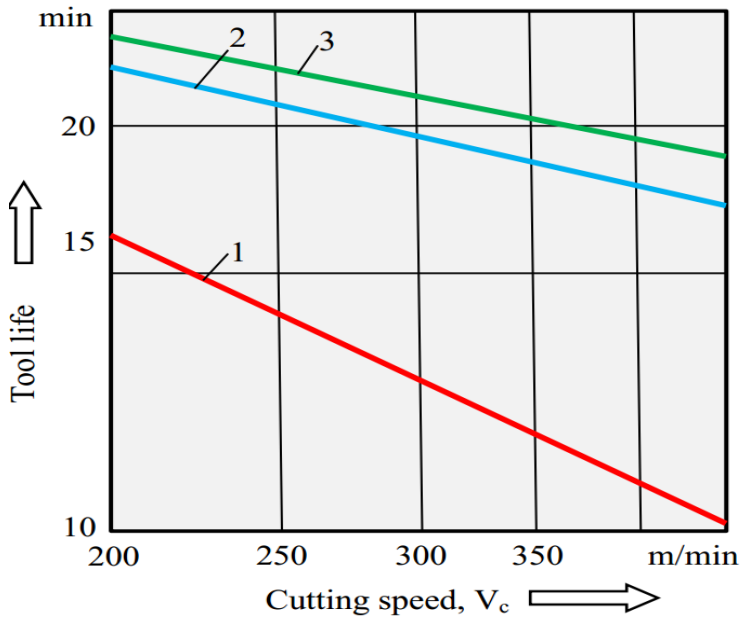


**Figure 12.** Dependence of "cutting speed - tool life" for tools made of carbide grade TT10K8B when milling steel C45 with  $a_p = 2.0$  mm;  $f = 0.3$  mm/rev: 1 - uncoated; 2 - NMCC of Ti-TiN-(NbZrTiCr)N (standard MeVVA technology); 3 - NMCC of Ti-TiN-(NbZrTiCr)N (FCVAD technology)

The maximum increase of tool life is shown by inserts with developed NMCC based on Ti-TiN-(NbZrTiCr)N (FCVAD technology) (see Fig. 10-13 curves 3).

For this system, this study confirmed the data obtained by many researchers [1-4][6][38-40] about increase in the tool efficiency with wear-resistant coatings reached after increase of cutting speed. An increase in the tool life (3 to 6 times) is shown by carbide inserts with developed NMCC. This is achieved by integration of the effects of reduction of the thermo-mechanical stresses and simultaneous favorable transformation of the contact and tribological processes during cutting.

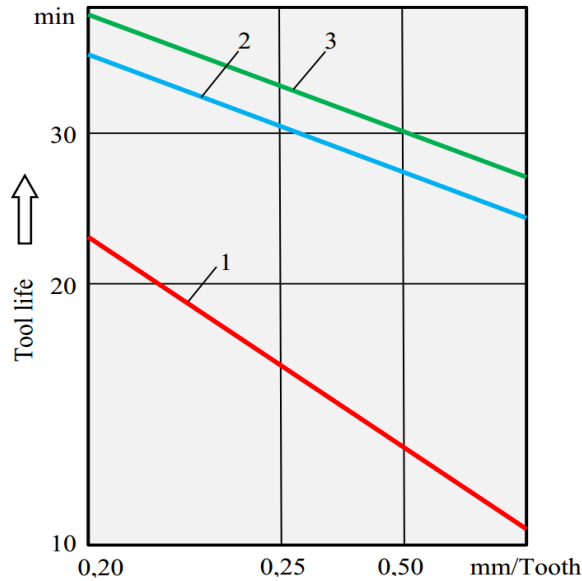


**Figure 13.** Dependence of "cutting speed - tool life" for tools of carbide WC10XOM when milling nickel alloy NiCr20TiAl with  $a_p = 2.0$  mm;  $v_c = 25$  m/min: 1- uncoated; 2 - NMCC of Ti-TiN-(NbZrTiCr)N (standard MeVVA technology); 3 - NMCC of Ti-TiN-(NbZrTiCr)N (FCVAD technology)

Another issue of particular interest is the results of the studies of cutting properties of WC10XOM carbide inserts with developed NMCC (standard MeVVA and developed FCVAD technology) for interrupted cutting (see Fig. 12, 13). Analysis of the presented data allows concluding the following. Milling process is accompanied by cyclic thermo-mechanical stresses, unsteady contact processes, and that fact significantly complicates the tool operation and intensifies its wear. However, there is an opinion of limited benefit of the use of NMCC for interrupted cutting which is overthrown by these new findings. Analysis of the results of verification tests of carbide tools in face milling shows that milling cutters equipped with carbide inserts with developed NMCC (FCVAD technology) had tool life 1.3-2.2 times higher than the tool life of milling cutters without coatings or with developed NMCC (FCVAD technology).

## 5. Conclusion

(a) This study has developed methods to produce modifying NMCC with nano-scale grain structure and thickness of sub-layers to significantly improve the cutting properties of tools made of carbides in continuous and interrupted cutting processes. The process of filtered cathodic vacuum-arc deposition (FCVAD) was developed to deposit NMCC, and this process increases the quality of NMCC due to almost complete (up to 90-95%) filtration of

macro/micro droplets of vapor-ion flow, blocking of electro-erosion etching of cutting edges and working surfaces of tools, formation of nano-dispersed grain structure of NMCC and nano-scale thickness of sub-layers of all its elements.

(b) Investigation of the composition and structure of NMCC deposited on carbide substrates with the use of the developed process of FCVAD allowed classifying the produced NMCC as nano-structured. In particular, the example of NMCC based on the system of Ti-TiN-(NbZrTiCr)N reveals that the outer layer (NbZrTiCr)N with thickness of 1.0  $\mu\text{m}$  has a nanolayer structure with thickness of sublayers of about 45-60 nm, and the intermediate layer (TiN) with total thickness of about 1.0  $\mu\text{m}$  also has the nano-scale layer structure with thickness of sub-layers of 45-60 nm, wherein the average value of all layers of the grain size is 5-10 nm.

(c) The studies of the properties of the inserts of different grades of carbides with developed NMCC showed their high efficiency. In longitudinal turning and face milling of steel C45 and nickel alloy NiCr20TiAl, the life of the carbide inserts with NMCC based on the system of Ti-TiN-(NbZrTiCr)N (FCVAD technology) was increased up to 5-6 times in comparison with the control inserts without coatings and up to 1.5-2.0 times in comparison with NMCC based on the system of Ti-TiN-(NbZrTiCr)N (standard MeVVA technology).

(d) The proposed technology can be used to enhance the tool life and reliability of cutting tools. Other important areas of application can be a corrosion-protective coating (including - for the medical products) and tribological coatings for friction pairs.

## **6. Acknowledgements**

This research was financed by the Ministry of Education and Science of the Russian Federation in the framework of the state order in the sphere of scientific activity (task No 2014/105, project No 385).

## 7. References

- [1] Vereschaka Anatoly S. Working capacity of the cutting tool with wear resistant . Moscow: Mashinostroenie; 1993. 245 p.
- [2] Vereschaka A.A., Vereschaka A.S., Mgaloblishvili O., Morgan M.N., Batako A.D. Nano-scale multilayered-composite coatings for the cutting . International Journal of Advanced Manufacturing Technology. 2014;**72**(1):303-317. DOI: 10.1007/s00170-014-5673-2
- [3] Vereschaka A.S., Vereschaka A.A., Migranov M.S.. The study wear resistance of the modified surface of the cutting tool. Applied Mechanics and Materials. 2014;**548-549**:417-421. DOI: 10.4028/www.scientific.net/AMM.548-549.417
- [4] Vereschaka A.A., Grigoriev S.N., Vereschaka A.S., Popov Yu. and Batako A.D.. Nano-scaled multilayered composite coatings for cutting tools operating under heavy cutting conditions. Procedia CIRP. 2014;**14**:239-244. DOI: 10.1016/j.procir.2014.03.070
- [5] Vereschaka A.S., Vereschaka A.A., Savushkin G.Ju., Sivenkov A.S.. Multilayered nano-scale coatings for cutting tool. Inorganic Materials: Applied Research. 2014;**5**(5):522-529. DOI: 10.1134/S2075113314050220
- [6] Volkhonskii A.O., Vereschaka A.A., Blinkov I.V., Vereschaka A.S., Batako A.D.. Filtered cathodic vacuum arc deposition of nano-layered composite coatings for machining hard-to-cut materials. International Journal of Advanced Manufacturing Technology. 2015;**81**(1-4)DOI: 10.1007/s00170-015-7821-8
- [7] Vereschaka A.S., Vereschaka A.A., Sladkov D.V., Akseenko A.Yu., Sitnikov N.N.. Control of structure and properties of nanostructured multilayer composite coatings applied to cutting tools as a way to improve efficiency of technological cutting operation. Journal of Nano Research. 2016;**37**:51-57. DOI: 10.4028/www.scientific.net/JNanoR.37.51
- [8] Moll E., Bergmann E.. Hard coatings by plasma-assisted PVD technologies: industrial practice.. Surface and Coating Technology. 1989;**37**:483-509. DOI: 10.1016/0257-8972(89)90085-6
- [9] Holleck H.. Basic principles of specific application of ceramic materials protective layers. Surface and Coating Technology. 1990;**43/44**:245-258. DOI: 10.1016/0257-8972(90)90078-Q
- [10] Fox-Rabinovich G.S., Kovalev A.I., Aguirrec M.H., Beake B.D., Yamamoto K., Veldhuis S.C., Endrinof J.L., Wainstein D.L., Rashkovskiy A.Y.. Design and performance of AlTiN and TiAlCrN PVD coatings for machining of hard to cut materials. Surface and Coating Technology. 2009;**204**(4):489-496. DOI: 10.1016/j.surfcoat.2009.08.021
- [11] Lierath F., Vereschaka A.. The main trends of vacuum-arc technology synthesis of multilayer coatings for cutting tool perfection. In: Proceedings of the IX Internationales Produktionstechnisches kolloquium PTK-98; 29-30 Oct. 1998; Berlin. 1998. p. 211-225.

- [12] Holleck H., Schier V.. Multilayer PVD coatings for wear protection. *Surface and Coatings Technology*. 1995;**76-77**(1):328-336. DOI: 10.1016/0257-8972(95)02555-3
- [13] Sheinman E.. Superhard coatings from nanocomposites. Review of foreign publications. *Metal Science and Heat Treatment*. 2008;**50**(11):600-605. DOI: 10.1007/s11041-009-9105-0
- [14] Bouzakis K.-D., Michailidis N., Skordaris G., Bouzakis E., Biermann R., M'Saoubi R.. Cutting with coated tools: Coating technologies, characterization method and performance optimization. *CIRP Annals - manufacturing Technology*. 2012;**61**(2):703-723. DOI: 10.1016/j.cirp.2012.05.006
- [15] Panckow A., Steffenhagen J., Lierath F.. Advanced coating architecture deposited by pulsed and filtered arc ion-plating. *Surface and Coating technology*. 2003;**163**:128-134. DOI: 10.1016/S0257-8972(02)00621-7
- [16] PalDey S., Deevi S.C.. Single layer and multilayer wear resistant coatings of (Ti,Al)N: a review. *Materials Science and Engineering A*. 2003;**342**:58-79. DOI: 10.1016/S0921-5093(02)00259-9
- [17] Vetter J., Burgmer W., Dederichs H., Perry A.. The architecture and performance of compositionally gradient and multi-layer PVD coatings. *Material Science Forum*. 1994;**163-165**:527-532. DOI: 10.4028/www.scientific.net/MSF.163-165.527
- [18] Cobine J.D.. Introduction to vacuum arc. In: Lafferty J.M., editor. *Vacuum arc: Theory and Application*. New York: John Wiley & Sons; 1980. p. 1-18.
- [19] Atamansky N., Dolotov J., Gorbunov V., Lunev V., Sablev L., Usov V.. Apparatus for metal evaporation coating. Patent US 3793179 A. 1974;
- [20] Beresnev N.M., Kopeikina M.Yu., Klimenko S.A.. Multicomponent and multilayer vacuum-arc coatings for cutting tool. *Voprosy atomnoi nauki i technics, Series: vacuum, pure materials, superconductors*. 2008;**1**:152-159.
- [21] Ecker G.. Theoretical aspects of the vacuum arc. In: J.M. Lafferty, editor. *Vacuum arc: Theory and Application*. New York: John Wiley & Sons; 1980. p. 228-320.
- [22] Steffens H.D., Mack M.K., Mohwald K., Reichel K.. Reduction of droplet emission in random arc technology. *Surface and coating Technology*. 1991;**46**:65-74. DOI: 10.1016/0257-8972(91)90150-U
- [23] Martin P.J., Bendavid A.. Review of the filtered arc processes and materials deposition. *Thin Solid Films*. 2001;**394**(1):1-14. DOI: 10.1016/S0040-6090(01)01169-5
- [24] Munz W.D.. Current industrial practices. The unbalanced magnetron: current status of development.. *Surface and Coating Technology*. 1991;**48**:81-94. DOI: 10.1016/0257-8972(91)90130-O
- [25] Grigoriev S.N., Melnik Y.A., Metel A.S., Panin V.V. Broad beam source of fast atoms produced as a result of charge exchange collisions of ions accelerated between two . *Instruments and Experimental Techniques*. 2009;**52**(4):602-608. DOI: 10.1134/S002044120904023X.
- [26] Aksenov I.I., Andreev A.A., Bren' A.A., et al. The coatings produced by the condensation of plasma flows in vacuum (method of condensation with ion bombardment). *Ukrainien Journal of Physics*. 1979;**24**(4):515-525.

- [27] Panckow A., Sladkov D., Singh P.K., Genzel C.. Low temperature metal ion implantation assisted deposition of hard coating. *Surface and Coatings Technology*. 2004;**188**(1):214-219. DOI: 10.1016/j.surfcoat.2004.08.027
- [28] Rauscheudach B., Sienz S., Six S., Gerlach J.. Synthesis of metal nitrides by low-energy ion assisted film growth. *Surface and Coating Technology*. 2001;**142-144**:371-375. DOI: 10.1016/S0257-8972(01)01273-7
- [29] Michalski A.J.. Structure and useful properties of multi-component titanium nitride obtained by pulse plasma deposition. *Journal of Material Science Letter*. 1991;**10**(9):503-505. DOI: 10.1007/BF00726919
- [30] Dodonov A., Bashkov V. Patent WO 98/45871 .1998
- [31] Boxman R.L., Goldsmith S. Principles and applications of vacuum arc coatings. *IEEE Transactions of Plasma Science*. 1989;**17**(5):705-712. DOI: 10.1109/27.41186
- [32] Panwar O.S., Mohd A. Khan, Satyendra Kumar, Basu A., Mehta B.R., Sushil Kumar, Ishpal. Effect of high substrate bias and hydrogen and nitrogen incorporation on spectroscopic ellipsometric and atomic force microscopic studies of tetrahedral amorphous carbon films. *Surface and Coatings Technology*. 2010; **205**(7): 2126-2133
- [33] Panwar O. S., Ttipathi R. K., Chockalingam S.. Chockalingam S. Improved nanomechanical properties of hydrogenated tetrahedral amorphous carbon films measured with ultra low indentation load. *Materials Express*. 2015; **5**(5):410-418
- [34] Tripathi R. K., Panwar O. S., Srivastava A. K., Ishpal, Mahesh Kumar, Sreekumar Chockalingam. Structural, Nanomechanical, and Field Emission Properties of Amorphous Carbon Films Having Embedded Nanocrystallites Deposited by Filtered Anodic Jet Carbon Arc Technique. *Journal of Nanoscience*. 2013; **2013**: 401710. DOI: 10.1155/2013/401710
- [35] Ahmed Abdulkadhim, Moritz to Baben, Tetsuya Takahashi, Volker Schnabel, Marcus Hans, Conrad Polzer, Peter Polcik, Jochen M. Schneider. Crystallization kinetics of amorphous Cr<sub>2</sub>AlC thin films. *Surface and Coatings Technology*. 2011; **206**(4): 599–603
- [36] Tripathi R.K., Panwar O.S., Srivastava A.K., Ishpal Rawal, Sreekumar Chockalingam. Structural, nanomechanical, field emission and ammonia gas sensing properties of nitrogenated amorphous carbon films deposited by filtered anodic jet carbon arc technique. *Talanta*. 2014;**125**: 276–283
- [37] Fox-Rabinovich G.S., Yamamoto K., Kovalev A.I., Veldhuis S.C., Ning L., Shuster L.S., Elfizy A.. Wear behaviour of adaptive nano-multilayered TiAlCrN/NbN coatings under dry high performance machining conditions. *Surface and Coatings Technology*. 2008;**202**(10):2015-2022. DOI: 10.1016/j.surfcoat.2007.08.067
- [38] Alexey Vereschaka, Anatoly Vereschaka, Dmitry Klauch, Dmitry Lytkin and Andre Batako.. High-efficiency machining of hard-to-cut materials used in heavy power engineering through the use of carbide tools with nano-scale multiphase coatings. *Procedia CIRP* 2016; **46**: 356–359. DOI: 10.1016/j.procir.2016.04.010
- [39] Vereschaka A.A., Vereschaka A.S., Popov A.Yu., Batako A. D., Sitnikov N.N. and Tverdokhlebov A.S.. Development of tool system for high-performance machining of products of railway rolling stock. *Procedia CIRP* 2016; **46**: 360–363. DOI: 10.1016/j.procir.2016.04.009

- [40] Vereschaka A.A., Vereschaka A.S., Bublikov Ju. I., Aksenenko A.Y., Citnikov N.N..  
Study of properties of nanostructured multilayer composite coatings of Ti-TiN-  
(TiCrAl)N and Zr-ZrN-(ZrNbCrAl)N. Journal of Nano Research. 2016;**40**:90-98. DOI:  
10.4028/www.scientific.net/JNanoR.40.90